EHL of an Elastic Ball Impact and Rebound from a Lubricated Elastic Coated Surface

Li-Ming Chu*, Chang-Jian, Cai-Wan**and Yuh-Ping Chang***

Keywords： EHL, Elastic coating, Elastic ball, Impact, Rebound

ABSTRACT

The pure squeeze elastohydrodynamic lubrication (EHL) motion of circular contacts with an elastic coating is investigated at impact and rebound process from a lubricated surface. The Reynolds, the ball motion, the rheology, and the elastic deformation equations must be solved simultaneously to obtain the transient pressure profiles (P), film shapes (H), elastic deformation, normal squeeze velocities (V_c) and accelerations (A_c). The first peak of central pressure (P_c) occurred at maximum impact force at impact end. In the rebound process, cavitation appears at the position near the edges of the dimple, the pressure spike (P_s) and the minimum film thickness (H_{min}) are developed at the edges of the dimple because of mass conservation, and closing moves towards the center of contact. At the end of rebound the P_s reached the contact center. The secondary peak is greater than the first peak. The effects of the elastic modulus (E) and thickness of coating (d) at impact and rebound process from a lubricated surface are discussed. Moreover, this research possesses academic innovation and value of industrial application, so it can be utilized by the industry to design and analyze mechanical components with coating.

INTRODUCTION

The extreme transient elastohydrodynamic lubrication (EHL) case consists of a mechanical element impacting a lubricant film. Therefore, the elastic dimple at the center of the contact region because of the impact squeeze effects occurred such as gear teeth, cams/followers, and rolling element bearings. Impact phenomenon exists widely in industrial machine elements. Surface coatings have long been used in industrial technologies, since they can reduce friction and wear, and thus improve the service life of mechanical components. Therefore, the characteristics of an elastic coating/elastic ball at impact and rebound process in the EHL region need to be further investigated.

The ball impacts a lubricant film has been widely studied experimentally by Wang et al (1992). They were the first to use an impact viscometer to study both the pressure distribution and the apparent viscosity of the oil film in EHL point contacts at pure squeeze motion. Safa and Gohar (1986) investigated pure impact problems using thin film transducers to measure the pressure in the contact region during impact process. They found that central pressure reached two peaks during the total impact period. The first peak corresponded to the stage of impact where the impact force reached its maximum. At the very end of the rebound process, immediately before the ball left the lubricated surface, a sharp contact center pressure peak was also found. Kaneta et al. (2007) observed the behaviours of point contact EHL films under impact loads using the optical interferometry technique. They found that when the initial impact gap is large, a central dimple is formed and the maximum film thickness (Hmax) occurs at the center of the contact region. When the initial impact gap becomes small, a periphery dimple is generated and the Hmax occurs at the contact periphery.

Yang and Wen (1991) and Chang (1996) analyzed the formation of the dimple in pure squeeze motion problems by numerical method. Dowson and Wang (1994) and Larsson and Högund (1995) analyzed the bouncing of an elastic ball on an oily plate. These analyses were restricted to normal motion in the first instance in order to develop the numerical technique and to relate the overall findings to the results presented by Safa and Gohar (1986). Venner et al. (2016) presented a formula to predict film thickness for the isoviscous and piezoviscous cases under pure impact revisited. They also tried to explain why the impact and the rolling contact produce pressure distributions and film thickness that

Paper Received June, 2017. Revised August, 2017. Accepted October, 2017. Author for Correspondence: Yuh-Ping Chang.

* *Professor, Department of Applied Science, Interdisciplinary Program of Green and Information Technology, National Taitung University, Taitung City, Taiwan 95092, ROC.*

** *Department of Mechanical and Automation Engineering, I-Shou University, Kaohsiung City, Taiwan 84001, ROC.*

*** *Department of Mechanical Engineering, Kun Shan University, Tainan City, Taiwan 71070, ROC.*

are so similar at circular contact.

To solve the coupled hydrodynamic equation and elasticity equation of an EHL problem, the elasticity modulus and thickness of the coating are important parameters. Many studies have treated the coating and contact surfaces as linear elastic isotropic materials. Elsharkawy and Hamrock (1995) explored the Newtonian EHL of an elastic coated surface on a rigid cylinder and rigid substrate using the deformation model developed by Johnson (1987). Jin (2000) presented a full numerical analysis of the EHL problem of a circular point contact involving a compliant layered surface firmly bonded to a rigid substrate under entraining motion. Jaffar (2008) derived a new set of explicit expressions for the contact pressure, total load, and penetration depth for the frictionless indentation problem of a spherical punch and a bounded thick elastic layer. Liu et al. (2007) developed a coating EHL model for point contacts by combining the DC-FFT algorithm for the elastic deformation of a coated surface with the unified mixed EHL model. Habchi (2015) presented a numerical investigation of the influence of thermo-mechanical properties of coatings on friction in elastohydrodynamic contacts. The results showed that friction in EHL contacts may be controlled by a suitable choice of surface coatings based on the thermal properties of their material. Chu et al. (2015) used the finite element method (FEM) to analyze and discuss the effects of a rigid sphere approaching a lubricated flat surface with an elastic coating on the elastic substrate on the transient EHL circular contact problems under constant load condition. Then, Chu et al. (2016) used the finite difference method (FDM) and the Gauss–Seidel iteration method to explore the effects of surface forces and coated layers on pure squeeze EHL under constant load condition. So far, no attempt has been made to study the squeeze film characteristics of EHL with coating at impact and rebound loading.

In this paper, pure squeeze EHL motion of circular contacts with coating is explored under impact and rebound condition. The finite difference method and the Gauss-Seidel iteration method are used to solve the transient Reynolds equation, the elasticity deformation equation, the ball motion equation, and the lubricant rheology equations simultaneously. The transient P and H during the impact and rebound processes under various operating conditions in the EHL regime are discussed.

THEORETICAL ANALYSIS

Modified Reynolds Equation

In EHL problems, two balls approaching each other may be treated as an equivalent ball approaching a plane. Figure.1 shows an elastic ball of radius R impacting and rebounding from a lubricated surface with an elastic coating. The lubricant is compressible. Under the usual assumption of EHL applicable to a thin film, the reduced momentum equations and the continuity equation governing the motion of the lubricant in polar coordinates can be obtained. Integrating the reduced momentum equations with the no-slip boundary conditions, the velocity components are then obtained. Substituting velocity components into the continuity equation and integrating across the film thickness with the boundary conditions of $v(r,h) = \partial h/\partial t$, the transient Reynolds equation in dimensionless polar coordinates can be derived as:

$$\frac{\partial}{\partial r}\left(\frac{\rho r h^3}{\mu}\frac{\partial p}{\partial r}\right) = 12 r \frac{\partial}{\partial t}(\rho h) \tag{1}$$

or in dimensionless form as:

$$\frac{\partial}{\partial X}\left(\frac{\bar{\rho} H^3 X}{\bar{\mu}}\frac{\partial P}{\partial X}\right) = \frac{8\pi X}{W}\frac{\partial}{\partial T}(\bar{\rho} H) \tag{2}$$

The radial coordinate, X, has its origin in the center of the contact. The boundary conditions for Eq. (2) are:

$$P(X \to \infty, T) = 0 \tag{3a}$$

$$\frac{\partial}{\partial X} P(0,T) = 0 \tag{3b}$$

$$P(R,T) \geq 0 \tag{3c}$$

When the pressure increases with time, the elastic deformation, and the effect of pressure on the viscosity cannot be neglected. It is the problem of pure squeeze motion in EHL.

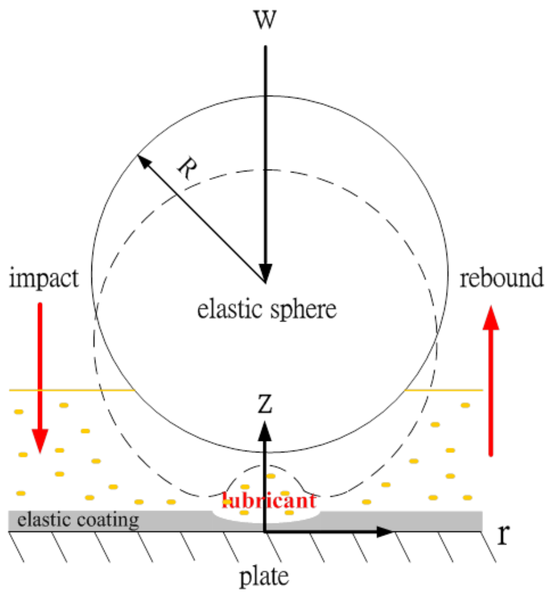

Fig. 1 Geometry of EHL of circular contacts at impact and rebound motion

Rheology Equations

At high pressure stage, the effects of the pressure on the viscosity and density cannot be neglected. The viscosity of the lubricant is assumed to be the function of pressure only. The relationship between viscosity and pressure used by Roelands et al. (1963) can be expressed as:

$$\bar{\mu} = \exp\{(9.67 + \ln \mu_0)[-1 + (1 + 5.1\times10^{-9} p)^{z'}]\} \quad (4)$$

where μ_0 is the viscosity at ambient pressure and z' is the pressure-viscosity index. According to Dowson and Higginson (1966), the relationship between density and pressure is given as:

$$\bar{\rho} = \frac{\rho}{\rho_0} = \frac{1 + 2.3\times10^{-9} p}{1 + 1.7\times10^{-9} p} \quad (5)$$

Elasticity Equation

At high pressure stage, the effects of the elastic deformation and pressure on the viscosity and density cannot be neglected. The film thickness in a nominal point contact elastohydrodynamic conjunction can be written as:

$$h(r,t) = h_0(t) + \frac{r^2}{2R} + \psi(r,t) + d(r,t) \quad (6)$$

The dimensionless film thickness between two elastic bodies in circular contacts can be expressed as:

$$H_i(X,T) = H_0(T) + \frac{X_i^2}{2} + \bar{\psi}_i(X,T) + \bar{d}_i(X,T) \quad (7)$$

To calculate the static deformation due to pressure distribution, influence coefficients D_{ij} are introduced. The deformation can thus be computed at discrete points i as a sum of the deformation contributions from all pressure points j :

$$\bar{\psi}_i = \sum_{j=1}^{n} D_{ij} P_j \quad (8)$$

where the influence coefficients, D_{ij}, are computed according to Yang (1991) and Larsson (1995). Within the frame of linear elasticity, the normal deformation of coated layer is given by Jaffar (2008)

$$\bar{d} = \frac{2\alpha R}{d b^2} \int_0^a \int_0^\infty [L(\omega) J_0(\frac{r\omega}{d}) J_0(\frac{s\omega}{d}) d\omega]\, p(s)\, s ds \quad (9)$$

where

$$L(\omega) = (2\kappa \sinh 2\omega - 4\omega)/(2\kappa \cosh 2\omega + 4\omega^2 + k^2 + 1)$$

$$\alpha = (1-\nu^2)/E\,, \quad \kappa = 3 - 4\nu$$

J_0 is the Bessel function of the first kind of order zero and ν is the Poisson's ratio.

Ball Motions

For the ball dropping case, as shown in Fig. 1, the equation of motion can be written as:

$$m\ddot{z}(t) = w_z(t) - mg \quad (10)$$

where z is a coordinate describing the position of the ball's center of gravity, and can be defined as:

$$z(t) = R + h_0(t) \quad (11)$$

Substituting Eq. (11) into Eq. (10) can be written as:

$$a_c(t) = \ddot{h}_0(t) = \frac{w_z(t)}{m} - g \quad (12)$$

or in dimensionless form

$$A_c(T) = \ddot{H}_0(T) = \frac{W_z(T)}{M} - \bar{g} \quad (13)$$

The initial conditions for Eq. (13) are

$$H_0(T=0) = H_{00} \quad (14a)$$

$$V_c(T=0) = V_{c0} \quad (14b)$$

The rigid separation and normal velocity of the ball's center in each time step can be determined as:

$$H_0^k = H_0^{k-1} + V_c^{k-1}\Delta T + A_c^{k-1}(\Delta T)^2/2 \quad (15)$$

$$V_c^k = V_c^{k-1} + A_c^{k-1}\Delta T \quad (16)$$

The relative impact force can be written as:

$$C_w = 3\int_0^\infty PXdX \quad (17)$$

To obtain the solution of the present isothermal EHL of circular contacts at impact loading problems, the Reynolds equation, the ball motion equation, the rheology equation, and the elastic deformation equation must be solved simultaneously.

RESULTS AND DISCUSSION

In this paper, the ball is assumed to accelerate continually from the initial lubricated film thickness ($h_{00} = 20\mu m$) with initial velocity ($v_{c0} = -0.1 m/s$) for all cases. Numerical solutions of film thickness (H) and pressure (P) in pure squeeze motion are calculated using the various input parameters presented in Table 1. The upper limit of the computational region, at the start, is chosen as $X_{max} = 10.0$. When more than half of the region is cavitation, the maximum analyzed region (X_{max}) reduces to half of its initial region, and so on, until $X_{max} = 2.5$. The grid is composed of 501 nodes, which are evenly distributed, in every calculating domain. The finite difference method (FDM) and the Gauss-Seidel iteration are employed to calculate H and P at each time step. A typical problem for d=0.1mm, $\mathrm{W} = 2.93\times10^{-8}$, $\mathrm{G} = 3500$, $E_b = 220\mathrm{GPa}$, $\nu_b = 0.3$, and $\nu_c = 0.3$ is solved.

Table 1 Computational data used in this paper.

Inlet viscosity of lubricant, Pa-s	0.04
Inlet density of lubricant, kg/m^3	846
Pressure viscosity coefficient (α), 1/GPa	15.91
Pressure-viscosity index (Roelands)	0.4836
Equivalent radius of elastic ball, m	0.02
Elastic modulus of coating, Pa	2.2×10^{15}~ 2.2×10^{18}
Elastic modulus of balls, Pa	2.2×10^{11}
Poisson's ratio of ball	0.3
Poisson's ratio of coating	0.3
Density of balls, kg/m^3	7850

The present algorithm solved a ball impacting and rebounding from a lubricated surface using the operation and initial conditions of Larsson and Höglund (1995). As shown in Figure 2, the numerical results for relative impact force are in good agreement with those obtained by Larsson and Höglund (1995). The discrepancies derive from the finer grids and calculation region varying with time in the present analysis.

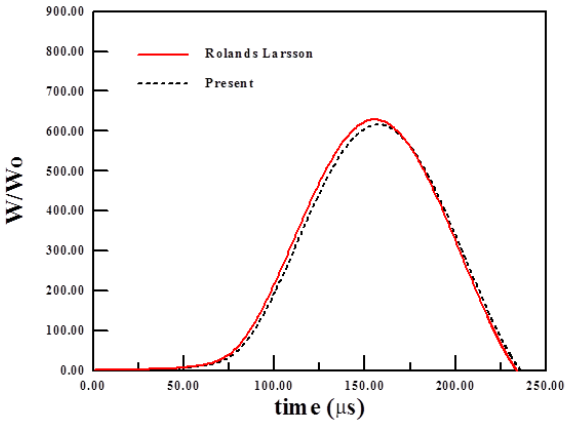

Figure 2. Compare the results of the numerical performed by Larsson and Höglund [1995] with the numerical results by using present method.

Figure 3. shows the relative change in the P and H for a ball approaching a flat surface lubricated with/without an elastic coating (d=0.1mm) for Newtonian lubricant, $m = 0.263kg$, and $v_{c0} = -0.1m/s$. When the ball started to impact the lubricated plate, the P increase gradually with the decreasing H, and the diameter of the dimple ($2b$) increases as the ball approaches the flat surface. The squeeze film action generates very large pressures in the lubricant and thus results in the formation of a central dimple in the elastic solids which lasts throughout the most impact period. The maximum pressure (P_{max}) and the maximum film thickness (H_{max}) occurred at central point of the contact region. When the ball begins to **rebound** from the lubricated surface, the pressure and the contact region decreased. The pressure spike (P_s) and the minimum film thickness (H_{min}) are developed at the edges of the dimple due to mass conservation, and closing moves towards the center of the contact. At the end of rebound, the P_s reached the contact center. The secondary peak could be greater than the first peak. The P_s and H with coating are smaller than that without coating, and the diameters of the dimples with coating are greater than that without coating at the same time during the impact process. Furthermore, the later the P_s and the H_{min} with coating are formed.

As described above, a second pressure peak occurred, forming at the dimple edge, moving rapidly toward the contact center at the end of the total impact time. Therefore, the P_c reached two peaks during the total impact period. It is seen from Figure 4. that the P_c increases gradually as the impact squeeze proceeds. The P_c reached first peak value, meantime, the ball begin to rebound. The P_c decreased as the rebound proceeds. In this paper, the primary peak pressures are formed about T=1.6813×10^9 (305.7μs) with coating, and T=1.6797×10^9(305.4μs) without coating, respectively. In addition, the times when the secondary peak pressure are formed about T=2.7181×10^9 (494.2μs) with coating, and T=2.3155×10^9 (421.0μs) without coating, respectively. Therefore, the later the first and the secondary pressure peaks are formed, the smaller the peak values are formed, and the longer the total impact time is for an elastic coating.

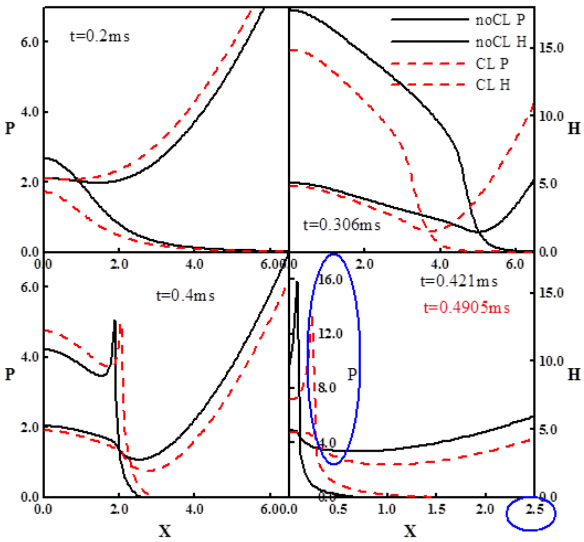

Figure 3. P and H versus X using two different models at different time.

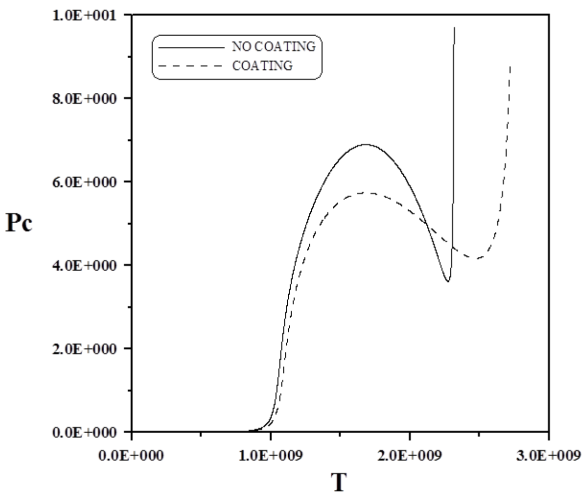

Figure 4. P_c versus T using two different models

At the initial stage, the H is thicker, and the pressure distribution is smaller. As the ball approaches the plate, the H becomes thinner, and the pressure distribution is large enough to cause elastic deformation of the ball. Figure 5. shows the relationship between H, the relative impact force (C_w) versus time with/without coating, respectively. It can be seen that the ball has reached the lubricant layer and begins to squeeze the lubricant film away at the initial impact stage. Since the pressure is low, the elastic deformation is very small, and the C_w rises slowly. When the central film thickness (H_c) reaches 5.2882 with coating and 5.5604 without coating, respectively, the pressure distribution rapid increases so that the elastic deformation effect is obvious. This figure also shows that the H_c, the H_{min} and the rigid separation (H_0) decrease with time, however, when the minimum value is reached, they gradually increase with time. Furthermore, the C_w increases with time, but when the maximum value is reached, it decreases with time. This phenomenon reveals the rebound. In the rebound process, cavitation appears at the position near the edges of the dimple. In addition, the H_c with coating is smaller than that without coating. The C_w with coating is smaller than that without coating. The H_{min} with coating is smaller than that without coating at the rebound stage. This is because the rigid base plate with the elastic ball and coating results in greater spring effect. This figure also shows a deviation of $\Delta T = 2.42 \times 10^7$ with coating and $\Delta T = 1.27 \times 10^7$ without coating, respectively, between the time of the maximum C_w and the minimum H_0. The phase shift is caused by the system including the damping and the elastic properties.

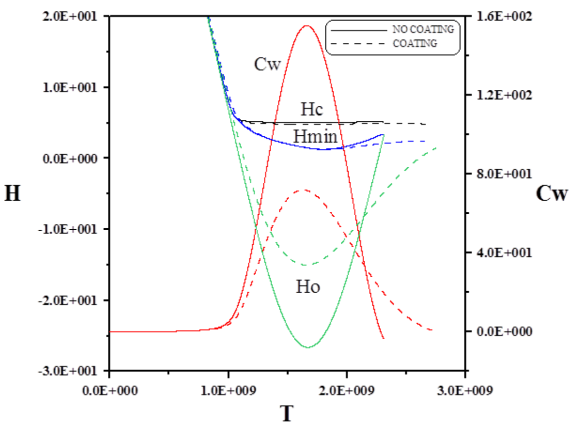

Figure 5. H and Cw versus T using two different models

Figure 6. shows the relationship between the squeeze velocity (V_c) and the squeeze acceleration (A_c) versus time before $T = 1.5 \times 10^9$. As the ball approaches the plate, the A_c decreases due to the reacting force applied by the oil film to the ball. However, the V_c increases due to the acceleration. Furthermore, in the high-pressure stage, Figure 7. shows the relationship between the V_c and the A_c with time during the total impact process. It can be observed that the counterforce given by the oil film to the ball exceeds the ball's weight. Acceleration of the ball's center from the counterforce gradually increases and the V_c of the ball's center gradually decreases, but C_w increases continuously due to the continuous squeezing process. When the counterforce created by the oil film increases to a peak value, acceleration also increases to a peak value and the V_c decreases to zero ($t \cong 2.2088 \times 10^9$ with coating and 1.6725×10^9 without coating, respectively), i.e., rebounding begins. During the rebounding process, A_c and C_w decrease gradually until the rebounding velocity reaches a peak, C_w approaches 1.0, and acceleration approaches zero. The figure also shows a deviation of $\Delta T = 5.803 \times 10^8$ with coating and $\Delta T = 1.43 \times 10^7$ without coating, respectively, between the peak value of the A_c and the V_c=0. This phase shift is also caused by the damping and elastic properties. In addition, it is seen from Figure 7 that the V_c and A_c with coating is smaller than that without coating.

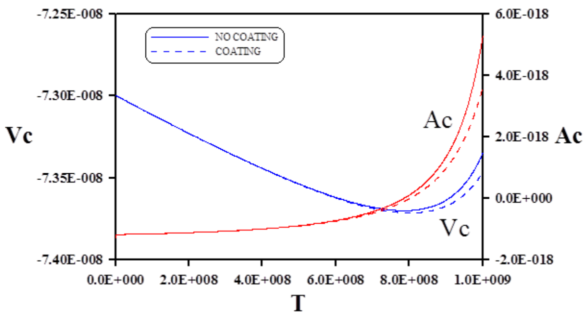

Figure 6. Vc and Ac versus T using two different models before $T = 1.0 \times 10^9$

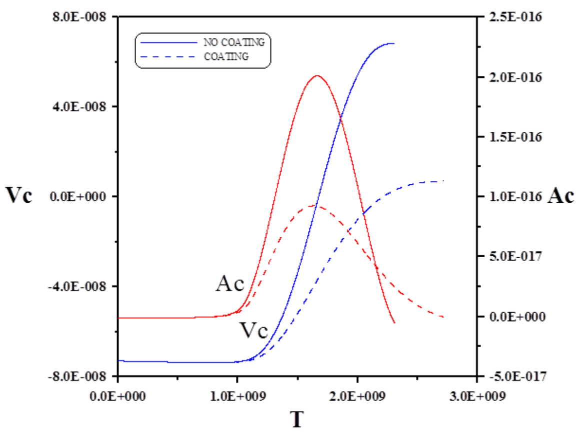

Figure 7. Vc and Ac versus T using two different models

Figure 8. shows the P_c versus time during the total impact process for different elastic modulus (E) and thickness (d) of coating. It can be seen that the greater the E, the greater the P_c, the earlier the first pressure peaks and the secondary pressure peaks, the greater the first pressure peak values and the secondary pressure peak values, and the shorter the total impact time. Furthermore, the smaller the coating thickness, the greater the P_c, the earlier the first pressure peaks and

the secondary pressure peaks, the greater the first pressure peak values and the secondary pressure peak values, and the shorter the total impact time.

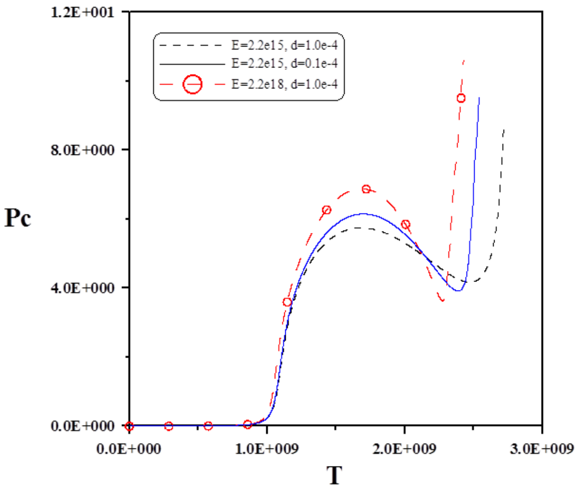

Figure 8. P_c versus T using different E and d.

Figure 9 shows the H and the C_w versus time during the total impact process for different E and d. It can be seen that the greater the E, the greater the H_c and the greater the C_w. The H_{min} is almost same at the impact stage, but the greater the E, the greater the H_{min} at the rebound stage. Furthermore, the smaller the coating thickness, the greater the H_c and the greater the C_w. The H_{min} is almost same at the impact stage, but the smaller the coating thickness, the greater the H_{min} at the rebound stage. This figure also shows a deviation of $\Delta T = 1.10 \times 10^7$ for $E = 2.2 \times 10^8$ and $\Delta T = 1.71 \times 10^7$ for d=0.1mm, respectively, between the time of the maximum C_w and the minimum H_0.

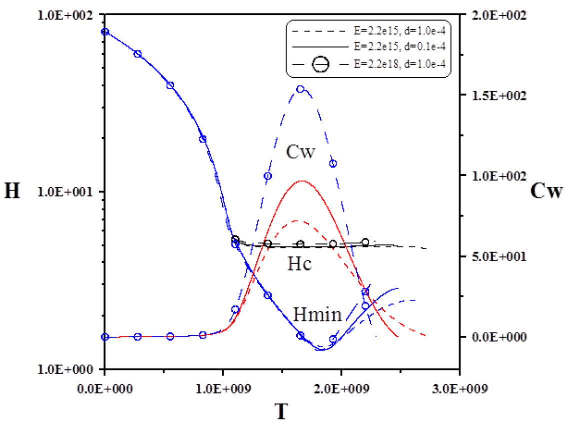

Figure 9. H and Cw versus T using different E and d

Figure 10. shows the V_c and the A_c versus time during the total impact process for different E and d. It can be seen that the greater the E, the greater the V_c and the A_c. The smaller the coating thickness, the greater the V_c and the A_c. The figure also shows a deviation of $\Delta T = 1.76 \times 10^7$ for $E = 2.2 \times 10^8$ and $\Delta T = 2.426 \times 10^8$ for d=0.1mm, respectively, between the peak value of the A_c and the V_c=0.

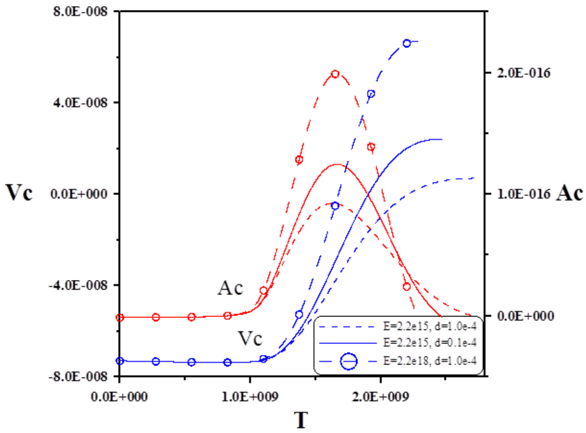

Figure 10. Vc and Ac versus T using different E and d

CONCLUSIONS

In this paper, the effects of elastic coating on pure squeeze EHL motion of circular contacts were explored at impact and rebound process from a lubricated surface. The main results can be summarized as follows:

1. The first peak of P_c occurred at maximum C_w and the secondary peak of P_c occurred at rebound end. The secondary peak is greater than the first peak.
2. In the rebound process, cavitation appears at the position near the edges of the dimple, the P_s and the H_{min} are developed at the edges of the dimple due to mass conservation, and closing moves towards the center of the contact. At the end of rebound the P_s reached the contact center.
3. The greater the E and the smaller the coating thickness, the greater the P_c , the earlier the first pressure peaks and the secondary pressure peaks, the greater the first pressure peak values and the secondary pressure peak values, and the shorter the total impact time.
4. The greater the E and the smaller the coating thickness, the greater the H_c, the greater the C_w at impact and rebound stage, and the greater the H_{min} at the rebound stage, and the smaller the phase shift between the time of the maximum C_w and the H_{min} is.
5. The greater the E and the smaller the coating thickness, the greater the V_c and the A_c, and the phase shift between the peak value of the A_c and the zero value of the V_c decreases.

ACKNOWLEDGMENT

The authors would like to express their appreciation to the Ministry of Science and Technology (MOST 104-2221-E-218-038, MOST 104-2221-E -214-051, MOST 104-2632-E- 214-002) in Taiwan, R. O. C. for financial support.

REFERENCES

Chu, L. M., Yu, C. C., Chen, Q. D., Li, W. L., "Elastohydrodynamic Lubrication Analysis of Pure Squeeze Motion on an Elastic Coating/Elastic Substrate System," Journal of Tribology, ASME, Vol. 137, No. 1, pp. 011503-1-011503-11 (2015).

Chu, L. M., Lin, J. R., Hsu, H. C., Chang, Y. P., "EFFECTS OF SURFACE FORCES ON SQUEEZE EHL MOTION BETWEEN ELASTIC BALL AND ELASTIC COATED SURFACE,"

Chang, L., "An Efficient Calculation of the Load and Coefficient of Restitution of Impact between Two Elastic Bodies with a Liquid Lubricant," ASME J. Applied Mech. Vol. 63, No. 2, pp. 347-352 (1996).

Dowson, D., and Higginson, G. R., Elastohydrodynamic Lubrication, Pergamon, Oxford, UK, (1966).

Dowson, D. and Wang, D., "An Analysis of the Normal Bouncing of a Solid Elastic Ball on an Oily Plate," Wear, Vol. 179, No. 1-2, pp. 29-37 (1994).

Elsharkawy, A. and Hamrock, B., "Elastohydrodynamic Lubrication of Elastomeric-Coated Surfaces in Line Contact," Proc. Inst. Mech. Eng. Part J.-J. Eng. Tribol., Vol. 209, No. 2, pp. 119-130 (1995).

Habchi, W., "Influence of thermo-mechanical properties of coatings on friction in elastohydrodynamic lubricated contacts," Tribology International, Vol. 90, pp. 113-122 (2015).

Johnson, K. L., Contact Mechanics, Cambridge university press, Cambridge, UK, (1987).

Jin, ZM., "Elastohydrodynamic lubrication of a circular point contact for a compliant layered surface bonded to a rigid substrate, part 1: theoretical formulation and numerical method," Proc. Inst. Mech. Eng. Part J.-J. Eng. Tribol., Vol. 214, No. 3, pp. 267-279 (2000).

Jaffar, M. J., "On the frictionless axi-symmetric contact of a thick elastic layer and the associated squeeze film problem," Proc. Inst. Mech. Eng. Part J.-J. Eng. Tribol., Vol. 222, No. 1, pp. 61-68 (2008).

Kaneta, M, Ozaki, S, Nishikawa, H, Guo, F., "Effects of impact loads on point contact elastohydrodynamic lubrication films," Proc Inst Mech Eng Part J: J Eng Tribol., Vol. 221, No. 3, pp. 271-278 (2007).

Larsson, R. and Högund, E., "Numerical Simulation of a Ball Impacting and Rebounding a Lubricated Surface," ASME J. Tribol., Vol. 117, No. 1, pp. 94-102 (1995).

Liu, Y., Chen, W. W., Zhu, D., Liu, S., and Wang, Q. J., "An Elastohydrodynamic Lubrication Model for Coated Surfaces in Point Contacts," J. Tribol.-Trans. ASME, Vol. 129, No. 3, pp. 509-516 (2007).

Roelands, C. J. A., Vlugter, J. C., and Watermann, H. I., "The viscosity temperature pressure relationship of lubricating oils and its correlation with chemical constitution, " ASME J. Basic Eng., Vol. 85, No. 4, pp. 601-607 (1963).

Safa, M. M. A. and Gohar, R., "Pressure Distribution Under a Ball Impacting a Thin Lubricant Layer," ASME J. Tribol., Vol. 108, No. 1, pp. 372-376 (1986).

Venner, C.H., Wang, J., Lubrecht, A.A., "Central film thickness in EHL point contacts under pure impact revisited," Tribology International, Vol. 100, pp. 1-6 (2016).

Wong, P. L., Lingard, S. and Cameron, A., "A. The high pressure impact microviscometer," STLE Tribology Trans., Vol. 35, No. 3, pp. 500-508 (1992).

Yang, P. R., and Wen, S. Z., "Pure Squeeze Action in an Isothermal Elastohydrodynamic Lubricated Spherical Conjunction, Part 2: Constant Speed and Constant Load Results," Wear, Vol. 142, No. 1, pp. 17-30 (1991)

NOMENCLATURE

a_c	normal acceleration of the ball's center $(\mathrm{m/s^2})$
A_c	dimensionless normal acceleration of the ball's center, $a_c R\mu_0^2/E'^2 b^2$
b	reference Hertzian radius at load w_0 (m), $\mathrm{b} = \mathrm{R}(1.5W)^{1/3}$
C_w	relative impact force, w/w_0
d	coating thickness (m)
D_{ij}	influence coefficients for deformation calculation
E'	equivalent elastic modulus (Pa)
E	elastic modulus of coating (Pa)
g	acceleration of gravity $(\mathrm{m/s^2})$
$\bar{g}$	dimensionless acceleration of gravity , $\mathrm{g}\mu_0^2 R/E'^2 b^2$
G	dimensionless material parameter, $\alpha E'$
h	film thickness
h_0	rigid separation
h_c	central film thickness
h_{min}	minimum film thickness
H	dimensionless film thickness, hR/b^2
K	constant in Reynolds equation, $8\pi/W$
m	mass of ball (kg)

p	pressure (Pa)
p_c	central pressure (Pa)
p_h	reference Hertzian pressure at load w_0 (Pa), $P_h = E(1.5W)^{1/3}/\pi$
P	dimensionless pressure, p/p_h
r	radial coordinate (m)
R	ball radius (m)
t	time (sec)
T	dimensionless time, tE'/μ_0
ΔT	dimensionless time step
v_c	normal velocity of the ball's center (m/s)
v_{c0}	initial normal velocity of the ball's center
V_c	dimensionless normal velocity of the ball's center, $v_c\mu_0 R/E'b^2$
w	reference load, $w=mg$ (N)
w_z	impact force (N)
W	dimensionless reference load, $w/E'R^2$
W_z	dimensionless impact force, $w_z/E'R^2$
X	dimensionless radial coordinate, r/b
z	axial coordinate
z'	pressure-viscosity index
μ	viscosity of lubricant (Pa-s)
μ_0	viscosity at ambient pressure (Pa-s)
$\bar{\mu}$	dimensionless viscosity, μ/μ_0
ρ	density of lubricant (kg m^{-3})

具彈性鍍層表面受彈性球衝擊及反彈之彈液動潤滑研究

朱力民
教授國立臺東大學應用科學及綠色資訊學位學程

張簡才萬
教授 義守大學機械與自動化工程學系

張育斌
教授 崑山科技大學機械工程系

摘要

本研究探討牛頓潤滑劑在具鍍層接觸表面受衝擊及反彈之彈液動潤滑問題。將暫態雷諾方程式、運動方程式、流變方程式及彈性變形方程式耦合起來，求解此一非線性微分方程組，可解得暫態的壓力分佈、油膜分佈、彈性變形、擠壓速度與擠壓加速度。結果顯示，中心壓力隨時間變化的第一峯值發生在衝擊結束即產生最大衝擊力時，在反彈過程中，由於質量必須守恆，所以空蝕現象會發生在內凹邊緣處附近，而壓力尖突及最小油膜都會發生在內凹邊緣處，且會隨著時間增加而向中心接近，當壓力尖突到達接觸中心處時，反彈結束，此壓力尖突也為中心壓力的第二峯值，第二峯值大於第一峯值。本研究也討論鍍層的彈性模數及厚度對衝擊及反彈過程彈液動潤滑的影響。本研究具有學術創新性，並可供工業界設計分析具鍍層的機械元件時使用，具產業應用價值。